Electronic Supplementary Material (ESI) for Analyst.
This journal is © The Royal Society of Chemistry 2021

Supplementary Information (SI)

3D Imaging for Single Bacterial Cell Using Surface-enhanced Raman Spectroscopy with Multivariate Curve Resolution Model

Wenjing Liu[b], Chuanbo Jing[c], Xiaowei Liu[b], Jingjing Du[a]*

[a]State Key Laboratory of Environmental Chemistry and Ecotoxicology, Research Center for Eco-Environmental Sciences, Chinese Academy of Sciences, Beijing 100085, China

[b]Key Laboratory for Environmental Factors Control of Agro-product Quality Safety, Ministry of Agriculture and Rural Affairs, Agro-Environmental Protection Institute, Ministry of Agriculture and Rural Affairs, Tianjin 300191, China

[c]No. 4 Hospital, Jinan 250031, China

Tel: +86 10 6284 9358; Fax: +86 10 6284 9358

E-mail: jjdu@rcees.ac.cn

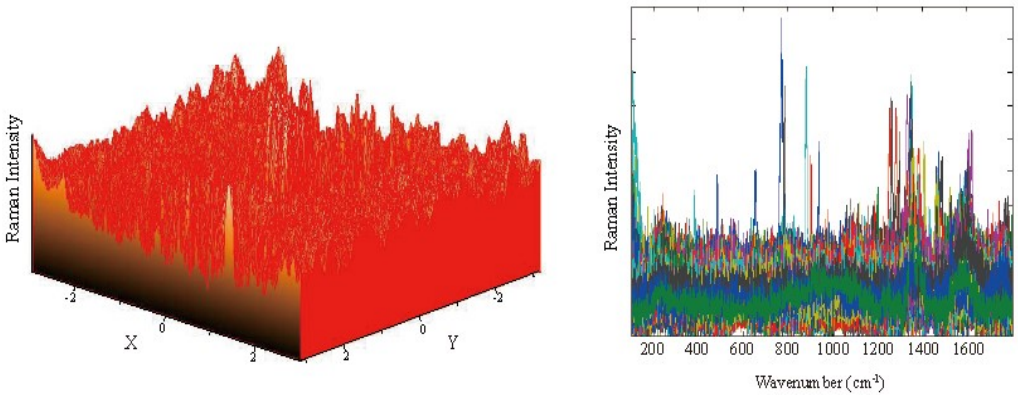

Figure S1. (a) Original Raman spectra of single cell mapping from x-axis and y-axis. (b) overlap of Raman spectra from all pixels.

Cluster analysis method segments the spectra from the Raman mapping dataset into clusters of similar spectra according to their resemblance. Hierarchical clustering analysis (HCA) and divisive clustering analysis (DCA), as the two widely-used nested clustering methods, were applied to the same spectral dataset for single cell. HCA method initially assumes that each spectrum forms a cluster and then iteratively nests the most similar clusters together. Each HCA component spectrum corresponds to the location indicated by the corresponding color in the SERS spectral map. Figure S2 shows that the single cell could be clearly differentiated from the background and HCA comp1 spectrum reveals the background information. Meanwhile, the image of the scores on HCA comp3 was nearly same with the cell image. However, other HCA components display similar characteristic peaks and represent the information of strong individual signal spots in SERS spectral map. Thus, HCA components was unable to give the abundant and various biomolecule information.

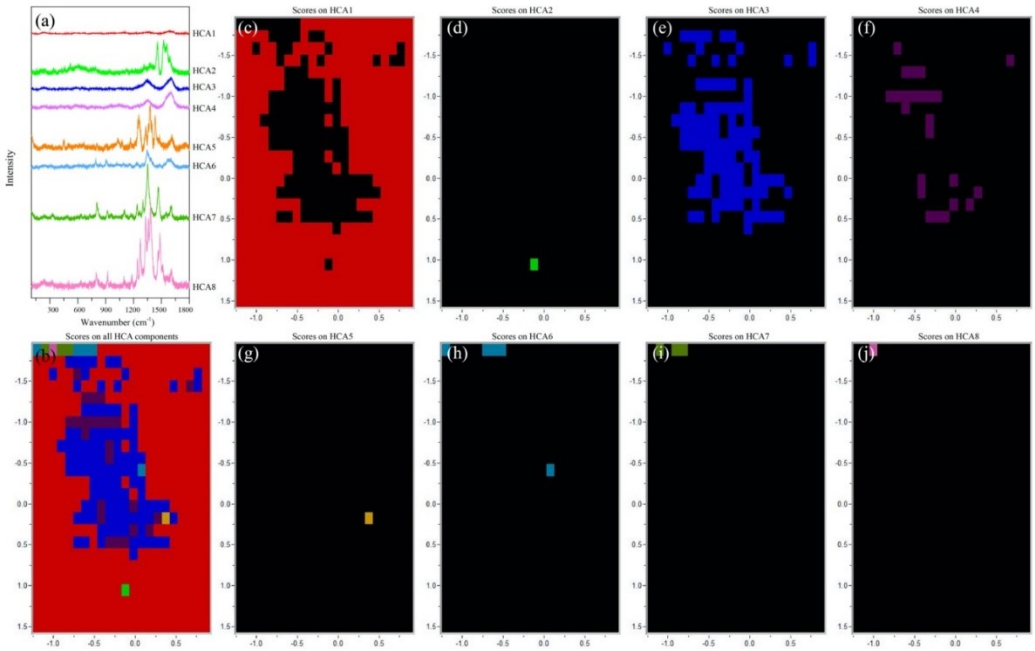

Figure S2. HCA analysis of SERS mapping from single cell. (a) Loading of HCA components calculated from Raman spectral dataset of single cell. (b) The false color map of the single cell constructed by HCA analysis. (c-j) The distribution of each HCA component spectrum is built on its corresponding scores.

DCA method assumes that all spectra are initially contained in a single cluster and then the most dissimilar data points are iteratively separated. As shown in Figure S4, the false color map constructed by DCA analysis could not represent the Raman imaging results. This is because that DCA model extracts different components information, neglecting the importance of the main and secondary components. Thus, the more effective statistic method was needed to analyze and fit the Raman maps of the single cell.

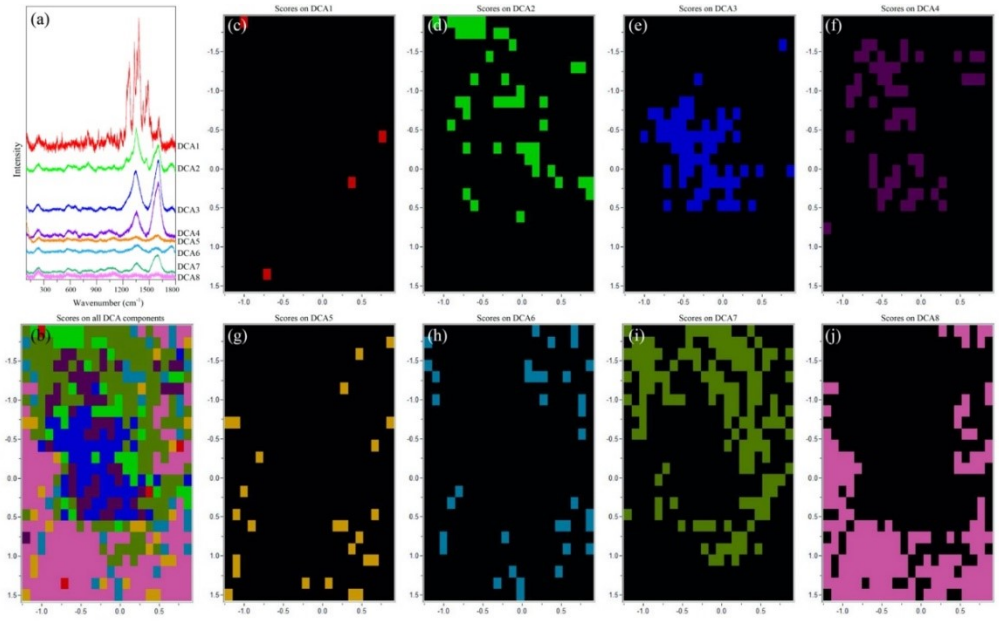

Figure S3. DCA analysis of SERS mapping from single cell. (a) Loading of DCA components calculated from Raman spectral dataset of single cell. (b) The false color map of the single cell constructed by DCA analysis. (c-j) The distribution of each DCA component spectrum is built on its corresponding scores.

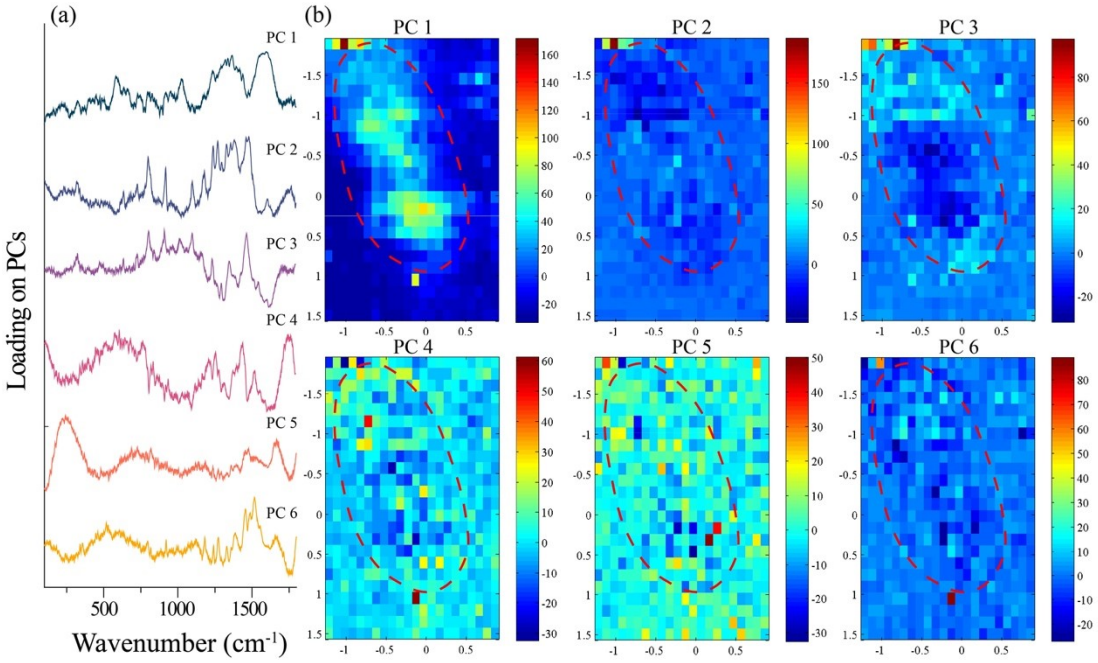

Figure S4. PCA analysis of SERS mapping from single cell with biosynthesized Ag NPs. (a) PC loadings calculated from Raman spectral dataset of single cell. (b) The distribution of each PC spectrum is built on its corresponding scores.

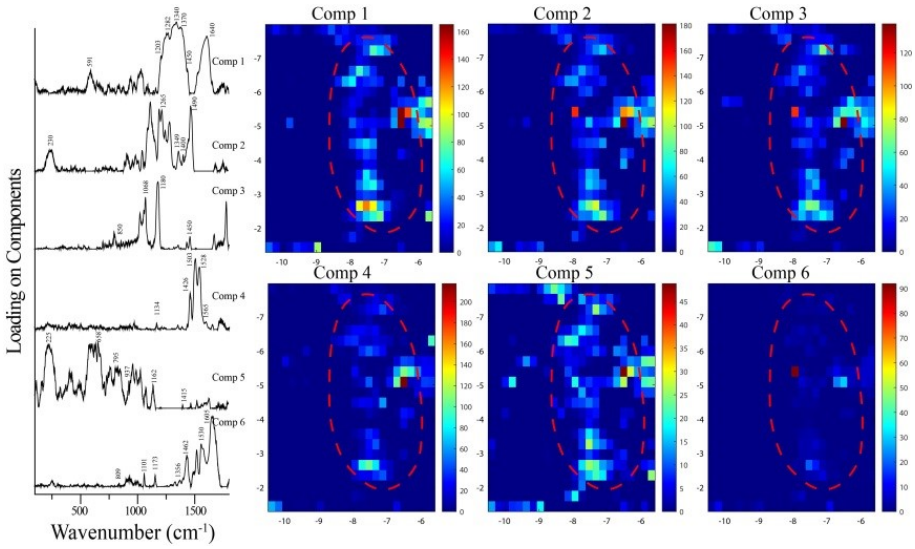

Fig. S5 MCR analysis of SERS mapping from single cell with biosynthesized Ag NPs. (Left) Component loadings calculated from Raman spectral dataset of single cell. (Right) The distribution of component spectra on corresponding scores.

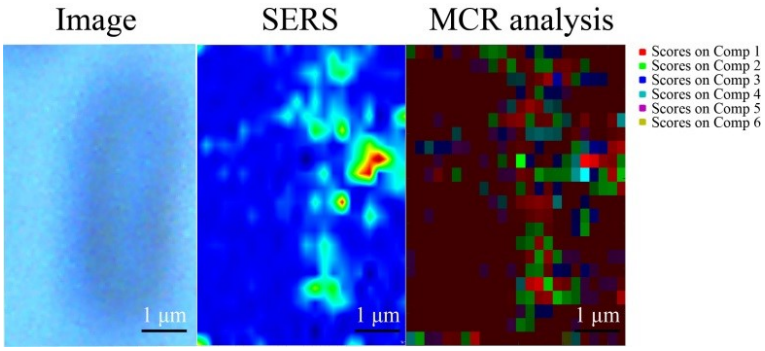

Fig. S6 Optical image, SERS mapping and MCR analysis of single IMH cell.

Table S1. Assignment of peaks in Raman spectra from spots of cell incubated with Ag(I)[1-18].

Band (cm^{-1}) Spot 1	**Band (cm^{-1}) Spot 2**	**Assignment**
220	239	Ag NPs aggregation, Ag-C, Ag-S or Ag-N vibration
466		Phenylalanine, Hydroquinone, Quinone, Fatty acids
	515	Serine, Saccharides, Citric acid
687		Glycine, Oxidized glutathione, Tryptophan, Citric acid
	708	Tryptophan, Saccharides,
	758	Tryptophan, Saccharides
817		Fatty acids, Serine, NAD^+

	822	Saccharides, Fatty acids, Glutathione, Valine, Tyrosine, Histidine
	891	Valine, Glutathione
947		Oxidized glutathione (C-COO^-), Valine, Proline, Saccharides, Coenzyme A
963		Valine, Serine, Histidine, Saccharides (Fucose, Cellulose)
	992	NADH, Nucleic acids (Cytosine, Uracil), Proline, Saccharides (arabinose)
	1124	Saccharides (Glucose, Cellulose, Trehalose), Glycine, Valine, Arginine, Coenzyme A
1237		Glutathione, Nucleic acids (Guanine, Uracil), Saccharides (Mannose)
1253		NAD^+, Riboflavin, Tryptophan, Histidine, Glutathione
	1332	Adenine, Glutathione, Coenzyme A, Valine, Arginine, Proline, Saccharides (D-(+)-trehalose, D-(+)-fucose)
	1392	NAD, Quinone, Nucleic acids (Guanine, Uracil), Citric acid
	1422	Coenzyme A, Acetoacetate, Glutamate, Tryptophan, Succinic acid
	1464	Riboflavin, Fatty acids, Cellulose, Alanine, Serine, Coenzyme A
	1527	Cytosine, riboflavin, glutamate
	1629	Glutathione, NAD^+ or $NADP^+$, Hydroquinone, Fumarate, Serine, Glycine

Table S2. Raman spectra band assignments of MCR components obtained from MCR analysis in Fig. 6 [1-18].

Component 1			Component 2			Component 3		
Band (cm^{-1})	**SERS in Literature**	**Assignment**	**Band (cm^{-1})**	**SERS in Literature**	**Assignment**	**Band (cm^{-1})**	**SERS in Literature**	**Assignment**
219		Ag NPs, Ag-S, Ag-Cl, Ag-N	1188		cytochrome C	855	855	glucose
591		L-Tryptophan				910	912	glucose
1203	1203	Amide III, CH_2 wagging	1265		saccharides	1062	1065	glucose
1215	1214	C-N Stretching, riboflavin	1329	1330	coenzyme A	1450	1456	glucose
1282	1282	fatty acids, cytosine	1348	1345	coenzyme A	1602	1605	coenzyme A
1319		Protein (CH_2 twi sting)	1397		cytochrome C			
1340	1340	amide III	1445	1446	coenzyme A			
1368		guanine, glutathione	1493	1500	riboflavin, cytochrome C			
1419		CH_2 scissoring vibration (lipid band)	1614	1615	cytochrome C			
1450	1449	CH_2 bending / deformation						

1562	1560	Tryptophan amide II						
1640	1639	amide I						
Component 4			**Component 5**			**Component 6**		
Band (cm^{-1})	**SERS in Literature**	**Assignment**	**Band (cm^{-1})**	**SERS in Literature**	**Assignment**	**Band (cm^{-1})**	**SERS in Literature**	**Assignment**
579		nucleic acids (uracil), tryptophan	230		Ag NPs	330		NADH
737	740	NAD (A ring)	658	660	glutathione	637		pyruvate
1115	1114	NADH/NAD	795	795	glutathione	729		coenzyme A
1426	1423	NAD				809	810	quinone
1447	1449	fatty acids	907	908	glutathione	918		proline
1527		riboflavin	1162		glutathione	1103		fatty acids
			1226	1227	Oxidized glutathione	1173	1172	quinone
			1416	1414	glutathione	1235	1233	quinone
			1735		citric acid	1302		nucleic acids, fatty acids
						1355	1354	quinone
						1468		fatty acids

Reference

[1] K. P. Sooraj, M. Ranjan, R. Rao, S. Mukherjee, SERS based detection of glucose with lower concentration than blood glucose level using plasmonic nanoparticle arrays, Appl. Surf. Sci. 447 (2018) 576-581.

[2] Y. Xia, P. Gao, X. Qiu, Q. Xu, S. Gan, H. Yang, et al., Aptasensor based on triplex switch for SERS detection of cytochrome c, Analyst, 137 (2012) 5705-5709.

[3] Genin Gary Huang, Xiao X. Han, Mohammad Kamal Hossain, Yasutaka Kitahama, Yukihiro Ozaki, A Study of Glutathione Molecules Adsorbed on Silver Surfaces Under Different Chemical Environments by Surface-Enhanced Raman Scattering in Combination with the Heat-Induced Sensing Method, Appl. Spectrosc. 64 (2010) 1100-1108.

[4] S. P. Chen, C. M. Hosten, A. Vivoni, R. L. Birke, J. R. Lombardi, SERS investigation of NAD+ adsorbed on a silver electrode, Langmuir, 18 (2011) 9888-9900.

[5] E. D. Puerto, A. Cuesta, S. Sanchez-Cortes, J. V. Garcia-Ramos, C. Domingo, Electrochemical SERS study on a copper electrode of the insoluble organic pigment quinacridone quinone using ionic liquids (bmimcl and tban) as dispersing agents, Analyst, 138 (2013) 4670-4676.

[6] A. Barhoumi, D. Zhang, F. Tam, N. J. Halas, Surface-enhanced raman spectroscopy of DNA, J. Am. Chem. Soc. 130 (2008) 5523-5529.

[7] S. Stewart, P. M. Fredericks, Surface-enhanced Raman spectroscopy of amino acids adsorbed on an electrochemically prepared silver surface, Spectrochim. Acta A Mol. Biomol. Spectrosc. 55 (1999) 1641-1660.

[8] F. Wei, D. Zhang, N. J. Halas, J. D. Hartgerink, Aromatic amino acids providing characteristic motifs in the Raman and SERS spectroscopy of peptides, J. Phys. Chem. B 112 (2008) 9158-9164.

[9] Z. Movasaghi, S. Rehman, I.U. Rehman, Raman spectroscopy of biological tissues, Appl. Spectrosc. Rev. 42 (2007) 493-541.

[10] J. De Gelder, K. De Gussem, P. Vandenabeele, L. Moens, Reference database of Raman spectra of biological molecules, J. Raman Spectrosc. 38 (2007) 1133-1147.

[11] Y.J. Xiao, W. Ting, X.Q. Wang, G. XiaoXia, Surface-enhanced near-infrared Raman spectroscopy of nicotinamide adenine dinucleotides on a gold electrode, J. Electroanal. Chem. 433 (1997) 49-56.

[12] N. Takahashi, T. Shinno, M. Tachikawa, T. Yuzawa, H. Takahashi, Time-resolved resonance

Raman, time-resolved UV–visible absorption and DFT calculation study on photo-oxidation of the reduced form of nicotinamide adenine dinucleotide, J. Raman Spectrosc. 37 (2006) 283-290.
[13] T. Deckert-Gaudig, E. Bailo, V. Deckert, Tip-enhanced Raman scattering (TERS) of oxidised glutathione on an ultraflat gold nanoplate, Phys. Chem. Chem. Phys. 11 (2009) 7360-7362.
[14] Y. J. Xiao, Y. F. Chen, X. X. Gao, Comparative study of the surface enhanced near infrared Raman spectra of adenine and NAD+ on a gold electrode, Spectrochim. Acta A 55 (1999) 1209-1218.
[15] R.H. Lahr, P.J. Vikesland, Surface-enhanced Raman spectroscopy (SERS) cellular imaging of intracellulary biosynthesized gold nanoparticles, ACS Sustain. Chem. Eng. 2 (2014) 1599-1608.
[16] R.A. Nyquist, D.A. Luoma, C.L. Putzig, Infrared and raman study of 1,4-benzoquinone and substituted 1,4-benzoquinones in dilute solutions, Vib. Spectrosc. 3 (1992) 181-210.
[17] H. Stammreich, T.T. Sans, Molecular Vibrations of Quinones. IV. Raman spectra of p-Benzoquinone and its centrosymmetrically substituted isotopic derivatives and assignment of observed frequencies, J. Chem. Phys. 42 (1965) 920.
[18] M. Kubinyi, G. Keresztury, Infrared and raman spectroscopic study of molecular interactions in quinhydrone crystals, Spectrochim. Acta A 45 (1989) 421.